Visualization of Solvent Diffusion in Polymers by NMR Microscopy with Radio-Frequency Field Gradients

Michel Valtier,[†] Piotr Tekely,[†] Laurent Kiéné,[‡] and Daniel Canet*,[†]

Laboratoire de Méthodologie RMN,[§] Université Henri Poincaré, Nancy 1, BP 239, 54506-Vandoeuvre les Nancy, Cedex, France, and CIRSEE, Lyonnaise des Eaux Dumez, 38, Rue du Président Wilson, 78230-Le Pecq, France

Received August 2, 1994; Revised Manuscript Received February 21, 1995[⊗]

ABSTRACT: NMR microscopy by radio-frequency field gradients is especially well suited for studying solvent penetration in polymers, due to the weak sensitivity of the method to magnetic susceptibility variations caused by object heterogeneities and to its ability to accommodate short transverse relaxation times better than the conventional imaging procedure by static field gradients. It is shown in this paper that distinct features of the swelling process can be easily observed by this method from two-dimensional NMR images and from the diffusion profiles provided by cross-sections through that image. A specific application of the method concerns the stretched PVC for which solvent diffusion and swelling are strongly anisotropic.

Introduction

In the last few years, it has been recognized that NMR imaging is a powerful tool for studying diffusion of solvents into polymeric materials.[1] Indeed, an extensive work on partially swollen PMMA was published by Weisenberger and Koenig[2,3] with the emphasis put on the case II and/or the Fickian character of the diffusional process. In these papers, the conditions of application of the conventional NMR imaging methods, based on static field gradients and spin echo techniques, were discussed. In particular, the authors established upper limits for the echo interval with respect to the transverse relaxation time T_2. They also considered the total measuring time in relation to the diffusional process itself which must remain sufficiently slow to prevent image distortions. By means of this technique, other studies have followed which include multicomponent diffusion,[4] sorption–desorption cycles,[5] and structural characterization of high molecular weight vinyl polybutadiene[6] and crossed-linked polystyrenes.[7] On the other hand, Mansfield et al.[8] published a thorough study of ingress of water in nylon, as a function of temperature and water pressure. Very recently Cody and Botto[9] have presented a detailed analysis of swelling kinetics by using standard NMR imaging. The results presented by these authors demonstrate that 2D NMR images together with the 1D shape of the concentration gradients reveal qualitatively the fundamental aspects of the transport mechanism. These examples attest that NMR imaging is the method of choice for studying the evolution of mobile components within a polymeric material, in contrast with other spectroscopic techniques which give access to microscopic information only at the surface of the object.

We wish to present here investigations of solvent penetration into polymers by an alternative NMR imaging method based on radio-frequency field gradients (B_1 gradients), as the continuation of a preliminary report on this subject.[10] This technique seems to be especially well suited for systems involving short transverse relaxation times.

Materials and Methods

Polymers under investigation were invariably studied in the following way: a rod, generally of rectanglular section, was cut from the raw material, immersed in the solvent for an appropriate time interval, thereafter removed from the solvent, and placed in a 9 mm i.d. tube for being examined by the NMR imaging procedure. In some instances, the polymeric sample was reimmersed in the solvent for allowing the diffusion process to continue. It is further assumed that in every case (i) desorption is negligible and (ii) the diffusion front advance is sufficiently slow to be smaller than one pixel in the final NMR image. Polymeric materials considered here include PVC (poly(vinyl chloride), PEhd (polyethylene high density), and stretched PVC. The solvents may be toluene, pentane, and trichloroethylene; they have been selected according to their ability to permeate the relevant polymeric material and because of their use in industrial applications.

The NMR experiment has been previously described in detail.[11] We shall just recall here its salient features. Essentially, it is based on projection-reconstruction procedures, the different projections being obtained by rotating the sample from one experiment to the other. Each experiment consists of (i) possibly selecting a slice along the vertical direction by means of the rf gradient of a saddle coil, used also for detecting the NMR signal[12] and (ii) spatial encoding by nutation of nuclear magnetization under an appropriate B_1 gradient along a horizontal direction; the gradient is delivered by a single turn coil (images presented in this paper have been obtained with a gradient of ca. 2 G/cm) and is applied in the form of short pulses whose lengths (typically 25 μs) determine the sampling rate. Nuclear magnetization is sampled between two consecutive gradient pulses, yielding a pseudo free induction decay, the Fourier transform of which represents the spin density profile associated with the relevant projection. These procedures yield two-dimensional images in principle free from magnetic susceptibility variation effects across the sample, in contrast with the conventional NMR imaging methods which employ static magnetic field gradients. Such variations exist in heterogeneous objects and create additional *static* gradients which add to the external gradient in conventional NMR imaging, producing image distortions. These magnetic susceptibility variations can also be viewed as inducing modifications of the Larmor frequency within the sample, leading to broadened lines. As far as imaging by B_1 gradients is concerned, spatial encoding arises from nutation (rotation of magnetization with respect to the radio-frequency field B_1) and is independent of line broadening within reasonable limits (of the order of 1–2 kHz).

* To whom correspondence should be addressed.
† Université Henri Poincaré.
‡ CIRSEE.
§ FU CNRS 008 (INCM) and URA CNRS 406 (LESOC).
⊗ Abstract published in *Advance ACS Abstracts,* May 15, 1995.

0024-9297/95/2228-4075$09.00/0

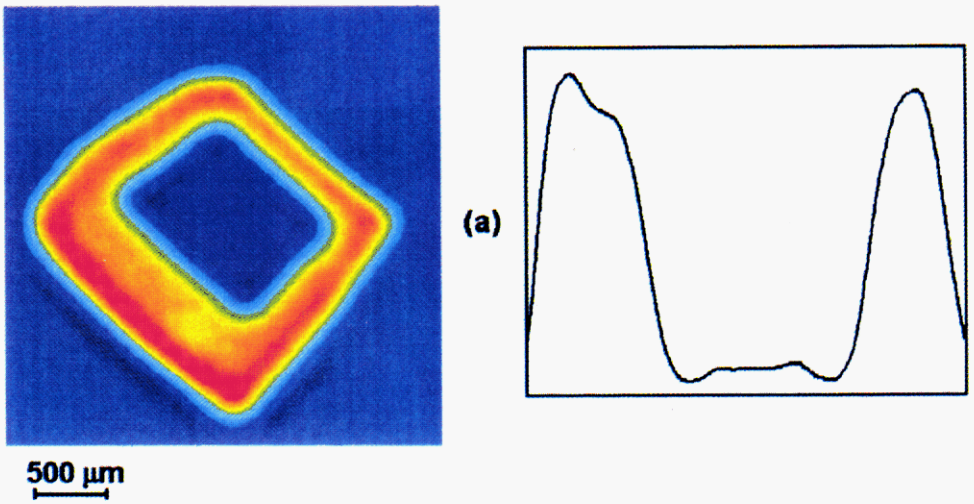

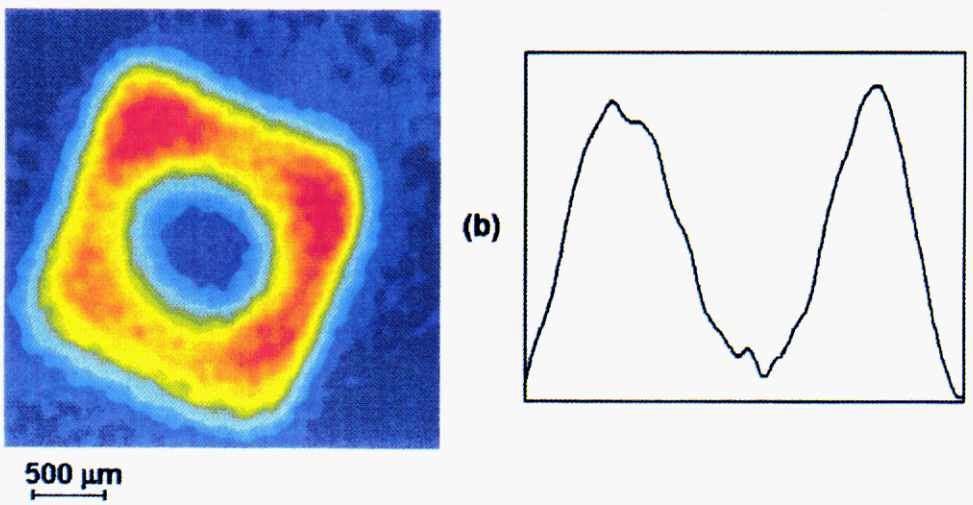

Figure 1. (a) Toluene in PVC and (b) *n*-pentane in PEhd. Left: two-dimensional images. The color goes from red (highest spin density) to dark blue (lowest spin density). Right: characteristic penetration profiles extracted from a cross-section through the corresponding image.

Moreover, because no spin echo is required, the method accommodates resonances possessing relatively short transverse relaxation times (T_2). In addition, because a nutation signal is acquired, the effective relaxation time $T_{1,2}$ affecting the imaging procedure is $1/T_{1,2} = (1/2)(1/T_1 + 1/T_2)$. In cases where $T_1 = T_2$ the effective relaxation time $T_{1,2}$ remains equal to the conventional relaxation times but reduces to $2T_2$ in the frequently encountered situation where the transverse relaxation time is much shorter than the longitudinal relaxation time T_1 ($T_2 \ll T_1$). This constitutes a further advantage of the B_1 gradient imaging since the penalty due to short transverse relaxation times, in terms of spatial resolution, is divided by a factor of 2.

All these features make NMR imaging by B_1 gradients well suited or the study of solvent penetration in polymers (samples necessarily heterogeneous with possibly, for the solvent, short transverse relaxation times), as confirmed by the examples presented in the following sections.

Visualization of the Diffusion Process

Case II diffusion is known to occur preferentially below the glass transition temperature (T_g). However penetration of solvent may induce a lowering of T_g so that the type of diffusion is difficult to predict. Case II diffusion is generally recognized by the rate of the diffusion front advance, which is linear as a function of time. Moreover, the diffusion front should be very sharp since it corresponds to an abrupt decrase of concentration between swollen and nonswollen regions of the polymer. Conversely, the so-called Fickian diffusion, described by the classical equation $\partial C/\partial t = D\Delta C$ (where Δ is the Laplacian, the equation being valid for isotropic diffusion) which accounts for the spatial variation of concentration C, should be accompanied by a smooth diffusion front and exhibit a front diffusion advance proportional to the square root of time. Finally, it can be mentioned that intermediate situations may occur.[13] We give below some examples demonstrating that different aspects of the transport phenomenon lead to distinct differences in 2D images and in the relevant cross-sections when observed by NMR microscopy with radio-frequency field gradients. Indeed, this technique leads to a good spatial resolution in spite of sample heterogeneities and short transverse relaxation times, in a measuring time sufficiently short for neglecting sample evolution during the NMR experiment.

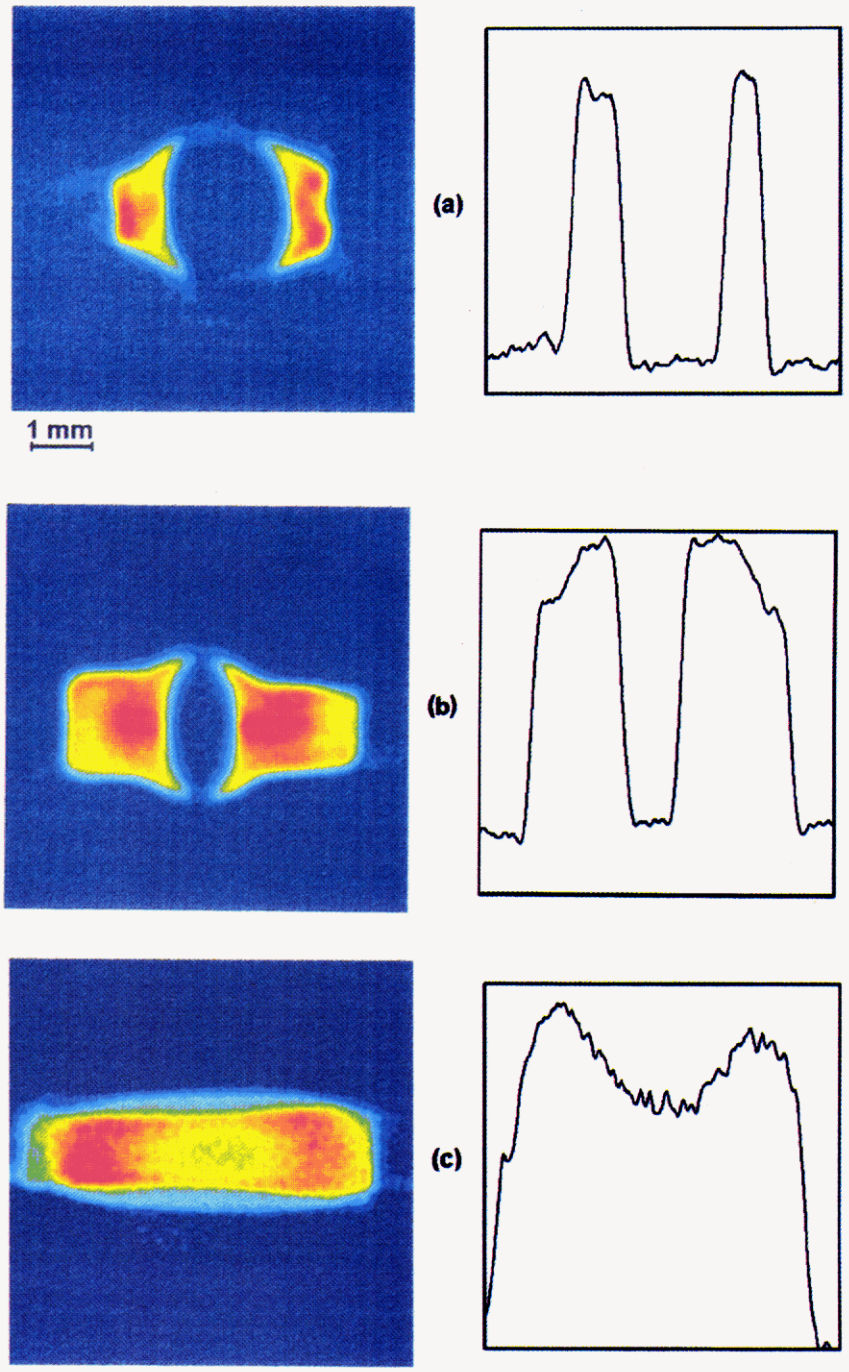

Figure 2. Solvent penetration in stretched PVC and swelling, after 14 h (a) and 30 h (b) of immersion in toluene, and final state after 30 h of immersion in trichloroethylene (c). Cross-sections (diffusion profiles) along the direction of preferential solvent penetration are shown on the right. The color scale is identical to the one for Figure 1.

A rod of PVC with roughly a square section was immersed in toluene for 30 h; a similar rod of PEhd was immersed in *n*-pentane for the same period of time. These samples were removed from the solvent and imaged according to methods described in the previous section. All operations were carried out at ambient temperature. Line widths, in the conventional NMR spectrum, were found to be approximately 200 Hz for toluene in PVC, as well as for *n*-pentane in PEhd. The two-dimensional images are displayed in Figure 1 along with a cross-section representing the profile of solvent penetration. Distinct differences may be observed in these 1D profiles: an abrupt decrease of concentration in the toluene–PVC system and a sort of exponential decrease in the case of *n*-pentane in PEhd. From weight gain as a function of time, it appears to assess, in both cases, the diffusion mechanism, although it has been claimed[13] that for PVC diffusion is generally a case II process whereas in PEhd the transport mechanism is known to be Fickian.

Our observations of a sharp diffusion front (commonly considered as a fingerprint of case II diffusion[1–5,9,13,14]) in the toluene–PVC system and an exponential solvent gradient directed into the core of the sample of PEhd (revealing the fundamental feature of Fickian diffusion[1–5,9,13,14]) seem to support the same conclusions.

A further difference, concerning the 2D contour of the diffusion front, exists between these two examples. For toluene in PVC the diffusion front reflects the outer shape of the object; this feature can be attributed to a linear progression of the solvent. Conversely, in the *n*-pentane–PEhd system, the diffusion contour is seen

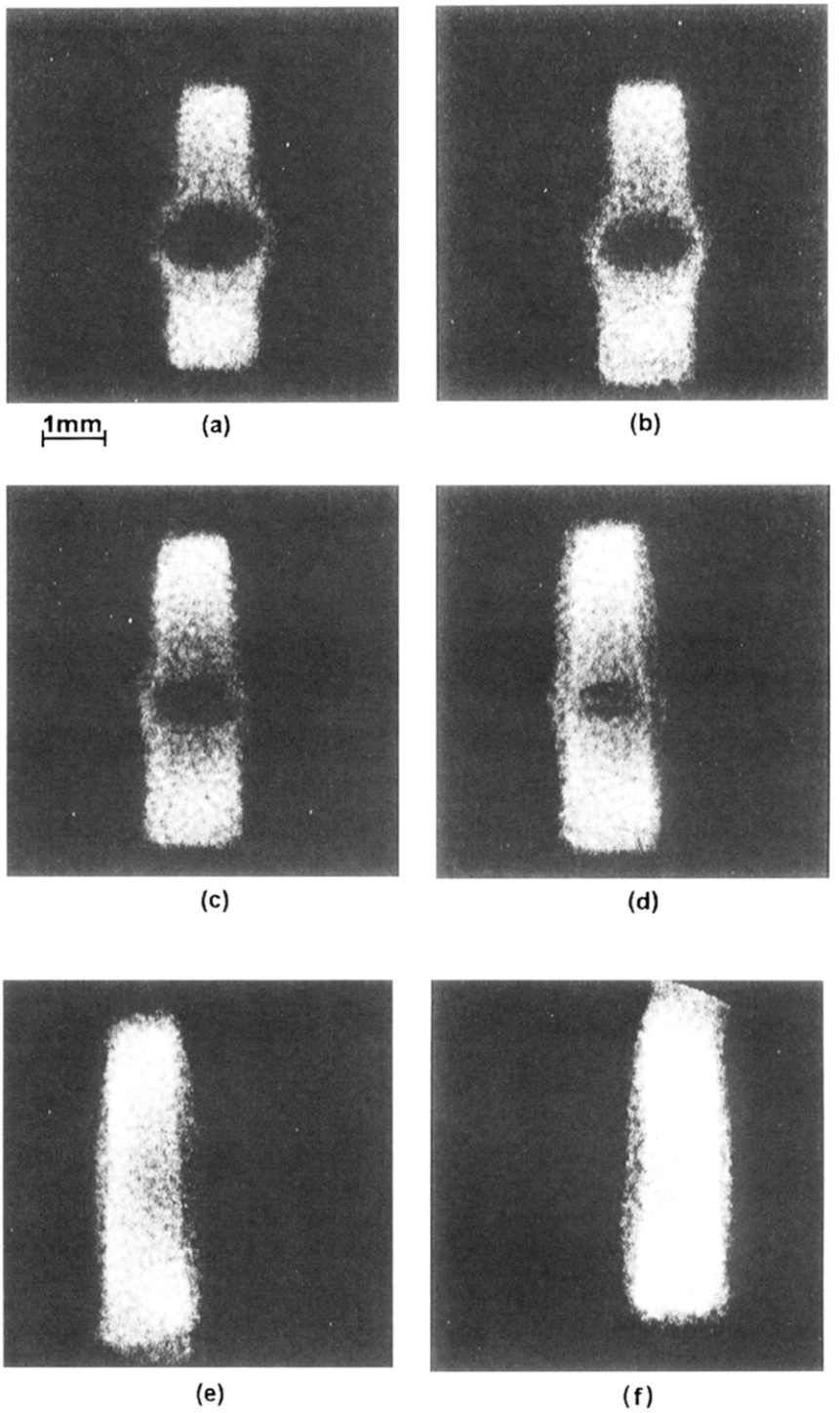

Figure 3. Diffusion of trichloroethylene in stretched PVC and the accompanying swelling process for the following times: (a) 18 h; (b) 20 h; (c) 22 h; (d) 24 h; (e) 26 h; (f) 28 h.

to be an almost perfect circle, in contrast with the squared outer shape of the object. Ths proves that memory of the object external faces is rapidly lost so that the solvent tends to advance within the material regardless of the initial constraints. These features suggest that the geometric figure associated with the diffusion front, as long as one is dealing with a non-cylindrical object, could constitute a further characterization of the diffusion process. To the best of our knowledge, this is the first time that such distinct features of the diffusion front have been observed experimentally in NMR imaging of swelling in glassy and rubbery polymers. Further investigations should be carried out on various systems to correlate the observed differences in the 2D contour of the diffusion front with the molecular and dynamic parameters[15] and with the fundamental characteristics of the transport mechanism process.[9,16-18]

Diffusion in Stretched PVC

Stretched PVC is obtained by heating a pipe of normal PVC above the polymer T_g and expanding it in a radial fashion; this results in a pipe of larger diameter whose mechanical properties are different along the radial and circular directions, respectively. For the present study, slices were cut from such a pipe, parallel to the pipe symmetry axis, so that they present two smooth sides (the outer and inner faces of the pipe) and two rough

sides (the sides which have been cut); the radial direction is therefore perpendicular to the smooth sides. The sample was immersed in the solvent (either toluene or trichloroethylene) for varying time intervals. Immersion was interrupted for short periods (ca. 40 min) for imaging purposes so that the whole diffusion and swelling processes could be followed almost in real time. The conventional NMR spectra exhibit line widths around 150 Hz for toluene and 50 Hz for trichloroethylene. They lead to the typical images shown in Figure 2. Because, at the onset, pieces of polymer were approximately of square section, it can be seen that the solvent penetrates preferentially by two sides, the smooth ones, and induces an elongation along a direction perpendicular to these two sides. This direction is precisely the radial direction of expansion. According to the duration of immersion, the central part of the rod is not reached by the solvent and remains nonswelled, leading to the appearance of an unaltered zone whose size diminishes gradually (Figure 2a,b). At the outset (Figure 2c), the polymer is almost fully imbibed and swelling along the radial direction is complete. In this polymer, the diffusion process is comparable with the one of toluene in normal PVC, as seen from the profiles shown in Figures 1a and 2a,b. The interpretation of this anisotropic diffusion process follows from the expansion of the material which can induce a preferred orientation of crystalline lamellae. This orientation would favor solvent penetration along the radial direction.

The diffusion and swelling processes of trichloroethylene in stretched PVC, after an initial immersion period of 18 h without any observation, are presented in Figure 3. Referring to Figure 2a,b, we observe that qualitatively trichloroethylene diffuses the same way as toluene and produces the same type of swelling. However, trichloroethylene diffuses faster due to its better ability to swell the polymer.

Finally, it can be mentioned that this two-dimensional stretching is difficult to detect by high-resolution solid state NMR techniques. Using carbon-13 $T_{1\rho}$ experiments, we found no significant changes in the relative proportions of the amorphous, crystalline, and intermediate regions between normal PVC[11] and stretched PVC either with or without solvent. Thus, at the molecular level, swelling does not seem to induce modifications in the amount of the different components. Conversely, the images of Figures 2 and 3 lend themselves to the visualization of the partial anisotropy of the system.

Conclusion

The present work has shown that NMR imaging by B_1 gradients is a viable method for obtaining details of solvent diffusion in polymers even in the case where line widths are of the order of several hundreds of hertz, corresponding to transverse relaxation times in the millisecond range. This is due (i) to the immunity of the method to static gradients originating from sample heterogeneities and (ii) to a bonus by a factor 2 when the transverse relaxation time is much shorter than the longitudinal relaxation time. Thus precise features, including diffusion profile and diffusion contour, could be obtained and used for characterizing microscopic and macroscopic aspects of the swelling process.

References and Notes

(1) Weisenberger, L. A.; Koenig, J. L. *Appl. Spectrosc.* **1989**, *43*, 1117 and references therein.
(2) Weisenberger, L. A.; Koenig, J. L. *Macromolecules* **1990**, *23*, 2445.
(3) Weisenberger, L. A.; Koenig, J. L. *Macromolecules* **1990**, *23*, 2454.
(4) Grinsted, R. A.; Koenig, J. L. *Macromolecules* **1992**, *25*, 1229.
(5) Grinsted, R. A.; Clark, L.; Koenig, J. L. *Macromolecules* **1992**, *25*, 1235.
(6) Rana, M. A.; Koenig, J. L. *Macromolecules* **1994**, *27*, 3727.
(7) Ilg, M.; Pfleiderer, B.; Albert, K.; Rapp, W.; Bayer, E. *Macromolecules* **1994**, *27*, 2778.
(8) Mansfield, P.; Bowtell, R.; Blackband, S. *J. Magn. Reson.* **1992**, *99*, 507.
(9) Cody, G. D.; Botto, R. E. *Macromolecules* **1994**, *27*, 2607.
(10) Maffei, P.; Kiéné, L.; Canet, D. *Macromolecules* **1992**, *25*, 7114.
(11) Maffei, P.; Mutzenhardt, P.; Retournard, A.; Diter, B.; Raulet, R.; Brondeau, J.; Canet, D. *J. Magn. Reson.* **1994**, *A107*, 40.
(12) Maffei, P.; Elbayed, K.; Retournard, A.; Brondeau, J.; Canet, D. *J. Magn. Reson.* **1991**, *95*, 382.
(13) Berens, A. R. *J. Vinyl Technol.* **1979**, *1*, 8.
(14) Alfrey, T.; Gurnee, E. F.; Lloyd, W. G. *J. Polym. Sci., Part C: Polym. Symp.* **1966**, *12*, 249.
(15) Vrentas, J. S.; Vrentas, C. M. *Macromolecules* **1993**, *26*, 1277; **1994**, *27*, 4684, 5570.
(16) Wu, J. C.; Peppas, N. A. *J. Appl. Polym. Sci.* **1993**, *49*, 1845.
(17) Peppas, N. A.; Wu, J. C.; von Meerwall, E. D. *Macromolecules* **1994**, *27*, 5626.
(18) Komoroski, R. A. *J. Polym. Sci., Polym. Phys. Ed.* **1983**, *21*, 1569.

MA946224H